future transportation

MDPI

Article

Investigating LiDAR Sensor Accuracy for V2V and V2P Conflict Detection at Signalized Intersections

Alireza Ansariyar * and Mansoureh Jeihani

Department of Transportation and Urban Infrastructure Studies, Morgan State University, Baltimore, MD 21251, USA; mansoureh.jeihani@morgan.edu
* Correspondence: alans2@morgan.edu

Abstract: This paper examined the accuracy of six installed LiDAR sensors at six different signalized intersections in Trois-Rivières City, Quebec, Canada. At each intersection, the crucial leading and following movements that cause vehicle–vehicle (V2V) and vehicle–pedestrian (V2P) conflicts were identified, and the LiDAR results were compared to crash reports recorded by police, insurance companies, and other reliable resources. Furthermore, the intersection crash rates were calculated based on the daily entering vehicle traffic and the frequency of crashes at each intersection. Convolutional Neural Networks (CNNs) were utilized over 970,000 V2V and V2P conflicts based on the post encroachment time (PET) and time-to-collision (TTC) safety assessment measures. Bayesian models were used to assess the relationships between different intersection characteristics and the occurrence of conflicts, providing insights into the factors influencing V2V and V2P conflict occurrences. Additionally, a developed image-processing algorithm was utilized to examine the conflicts' trajectories. The intersections' crash rates indicated that safety considerations should be implemented at intersections #3, #6, #4, #1, #5, and #2, respectively. Additionally, intersections #6, #4, and #3 were the intersections with the highest rates of vehicle–pedestrian conflicts. Analysis revealed the intricate nature of vehicle and pedestrian interactions, demonstrating the potential of LiDAR sensors in discerning conflict-prone areas at intersections.

Keywords: LiDAR sensor technology; V2V and V2P conflict; post encroachment time (PET); time-to-collision (TTC); signalized intersections; traffic safety

Citation: Ansariyar, A.; Jeihani, M. Investigating LiDAR Sensor Accuracy for V2V and V2P Conflict Detection at Signalized Intersections. *Future Transp.* **2024**, *4*, 834–855. https://doi.org/10.3390/futuretransp4030040

Academic Editor: Jaeyoung Lee

Received: 14 May 2024
Revised: 24 July 2024
Accepted: 2 August 2024
Published: 6 August 2024

1. Introduction

Traffic crashes and conflicts at signalized intersections are pervasive global concerns that have substantial societal, economic, and public health implications [1–3]. While signalized intersections aim to facilitate the orderly flow of traffic and enhance safety, they remain hotspots for collisions and near-miss crashes, with the potential for severe consequences. Understanding and mitigating the factors contributing to crashes and conflicts at signalized intersections are paramount for enhancing overall traffic safety [2,4,5]. Traditional approaches to this problem have heavily relied on post-crash data, such as police reports and insurance claims, which often lack detailed information about near-miss incidents or the contributing factors leading to crashes [6]. Moreover, the reliance on post-crash data can be problematic, as it may lead to a delayed response in implementing effective safety measures [7].

The advent of new technologies, particularly Light Detection and Ranging (LiDAR), offers a promising avenue for addressing these challenges [4,8]. LiDAR technology employs laser pulses to rapidly measure distances to surrounding objects and create high-resolution, three-dimensional point cloud maps of the environment. LiDAR technology is increasingly being harnessed to enhance our understanding of traffic dynamics and improve safety at signalized intersections by efficiently analyzing the trajectory of objects and recording the near-crash vehicle–vehicle, vehicle–bicyclist, and vehicle–pedestrian conflicts occurring [2].

By leveraging LiDAR technology, it is possible to capture real-time, high-fidelity data on vehicle trajectories, pedestrian movements, and the surrounding infrastructure. These data can be used to identify conflict points, near-miss crashes, and potential collision scenarios with unprecedented accuracy and detail [9]. Furthermore, LiDAR records data continuously, allowing for an analysis of long-term trends and an evaluation of the effectiveness of safety interventions over time [10]. In order to provide a comprehensive and accurate V2V and V2P conflict study at signalized intersections, explore the significance of leveraging LiDAR technology to record conflict data at signalized intersections, and compare the results with traditional crash reports, this paper aims to address the following key points for six signalized intersections in Trois-Rivières City, Quebec, Canada.

1. The real-time monitoring and analysis of V2V and V2P conflicts from January 2022 to June 2023 by collecting data from six installed LiDAR sensors at six different intersections.
2. An evaluation of safety interventions at six signalized intersections by highlighting the critical movements based on the frequency and severity of conflicts.
3. Providing PET and TTC surrogate safety assessment measures to investigate the recorded V2V and V2P conflicts.
4. Providing an intersection crash rate for each intersection based on the crash data analysis over a five-year period of investigation.
5. Comparing the results of the conflicts recorded by LiDAR and the crash reports analysis to specify the accuracy of critical movements obtained from both ways.

By bridging the gap between traditional crash reports and the real-world dynamics of signalized intersections, this research aims to contribute to a comprehensive traffic safety analysis. The integration of traditional crash reports with collected V2V and V2P conflict data obtained from LiDAR sensors at signalized intersections offers a comprehensive approach to improving safety for both vehicles and pedestrians. Traditional crash reports, often retrospective in nature, provide valuable insights into past collision occurrences. By combining these historical data with real-time, high-resolution V2V and V2P conflict information obtained through LiDAR sensors, a more proactive and comprehensive understanding of intersection safety dynamics emerges. This integrated approach allows for the identification of potential conflict areas before severe incidents occur, facilitating the design and implementation of targeted safety interventions. Leveraging this combined dataset provides a deeper understanding of near-miss events, which often precede actual crashes, enabling the early identification of hazardous scenarios and the development of proactive measures to mitigate risks. Ultimately, the utilization of LiDAR technology in this research in order to study traffic crashes and conflicts represents a paradigm shift in the field of traffic safety research, offering the potential to save lives, reduce injuries, and minimize the economic losses associated with intersection-related incidents. The remainder of this article is structured as follows: Section 2: Literature Review, Section 3: Materials and Methods, Section 4: Results, Section 5: Discussion, Section 6: Conclusions. Additional data analysis regarding the six signalized intersections can be found in Appendix A.

2. Literature Review

The analysis of conflicts at signalized intersections is a well-explored area in traffic safety research [1,2,4,8,11,12]. Various studies have utilized different methods and technologies to understand and mitigate conflicts between vehicles (V2V) and between vehicles and pedestrians [13,14]. Previous studies have concentrated on "conflict analysis at intersections" [15], "real-time conflict detection" [16], and "collaborative perceptions and advanced techniques" [17].

Several researchers have focused on conflict analysis at intersections to enhance traffic safety. A study by Yuan et al. in 2022 [18] utilized a microscopic traffic simulation to analyze the conflict patterns at urban intersections. This study provided insights into conflict scenarios, but relied heavily on simulated data, which might not capture the complexity of real-world interactions. Similarly, Essa and Sayed in 2018 [12] conducted an analysis of the conflict points at intersections using traditional crash data, which lack

the granularity required to understand near-miss events and real-time dynamics. Another study by Huang et al. in 2020 [10] applied statistical models to examine the frequency of conflicts at signalized intersections. While this approach highlighted significant factors contributing to conflicts, it did not leverage advanced sensing technologies for real-time conflict detection.

The integration of advanced sensing technologies such as LiDAR has shown promise in overcoming the limitations of traditional approaches. However, most existing studies have not fully utilized the potential of LiDAR for the continuous, real-time monitoring of conflicts. Studies by Xu et al. in 2018 [19], Sohail et al. in 2023 [20], Ansariyar et al. in 2023a, 2023b [2,4], and Bhattarai et al. 2024 [21] demonstrated the effectiveness of LiDAR in real-time traffic monitoring and conflict detection. These works highlighted the potential of LiDAR to provide accurate and timely data on vehicle and pedestrian movements, which are crucial for proactive traffic management. However, these studies did not fully explore the integration of LiDAR data with long-term crash statistics to comprehensively validate the technology's effectiveness.

Recent studies have proposed collaborative perceptions and advanced techniques to enhance conflict detection and resolution. The study by Anisha et al. in 2023 [1] introduced a framework for real-time conflict detection using V2V communication and by camera and LiDAR sensor fusion, which improved the accuracy of conflict prediction, but was limited by the need for high penetration rates. Similarly, studies by Olugbade et al. in 2022 [22], and Li et al. in 2023 [23] employed machine learning algorithms for conflict detection, showing potential in predictive analytics, but lacking integration with infrastructure-based sensing technologies like LiDAR.

The current study aims to address several key gaps in the literature. First, while previous studies have primarily relied on simulated or historical crash data, this research leverages real-time LiDAR data to capture the near-miss events and dynamic interactions at intersections. Second, the integration of CNN and Bayesian models provides a novel approach to assessing the relationship between intersection characteristics and conflict occurrences, offering deeper insights into the factors influencing V2V and V2P conflicts. Third, by comparing LiDAR-based conflict detection with traditional crash reports, this study validates the accuracy and effectiveness of LiDAR technology in real-world scenarios. Finally, the continuous monitoring capability of LiDAR enables long-term analysis, facilitating the evaluation of safety interventions and the identification of high-risk intersections over time.

3. Materials and Methods

PET is a critical parameter used in traffic engineering and safety analysis to assess potential conflicts and collisions at intersections [24]. PET refers to the period between the time when the first vehicle last occupied a position and the time when the second vehicle subsequently occupied that same position [2,4]. A PET equal to 0 indicates a collision and non-zero values indicate crash proximity. Higher PET values indicate a less severe crash, while lower PET values indicate a more severe crash [2,4].

TTC refers to the time it takes for a vehicle or object to collide with another vehicle, object, or obstacle in its path [25]. In other words, TTC is defined as the time remaining until two objects (e.g., vehicles) would collide if they continued on their current trajectories [26,27]. Understanding TTC is crucial, since it provides valuable insights into the potential for crashes and allows for timely preventive actions to be taken by drivers or automated safety systems. TTC can be estimated by the following:

1. Visual Estimation: Drivers estimate TTC based on visual cues such as the rate of approach of a nearby vehicle [26,28].
2. Sensor-Based Estimation: Sensors such as LiDAR, radar, and cameras are used in vehicles to estimate TTC [29,30].

3. Mathematical Models: Mathematical models, such as the time-to-collision equation, are utilized to estimate TTC based on the relative velocities and distances between objects [31,32].

LiDAR sensors capture precise spatial information, including vehicle positions, velocities, and orientations, enabling the extraction of detailed vehicle and pedestrian trajectories. LiDAR's ability to produce dense point cloud data assists in delineating vehicle and pedestrian movements, which form the basis for calculating PET and TTC values. By accurately measuring the distances between vehicles and pedestrians and capturing their movement dynamics, LiDAR sensors offer a comprehensive depiction of the spatial and temporal parameters necessary for determining potential conflicts. The rich and detailed data obtained from LiDAR technology enable the precise computation of PET and TTC values, considering factors such as relative speeds, distances, and the interactions of vehicles within the intersection space.

To predict vehicle and pedestrian trajectories, a CNN model was employed. The Algorithm 1 is detailed as follows:

Algorithm 1 CNN model to predict vehicle and pedestrian trajectories

Input: LiDAR data frames capturing vehicle and pedestrian movements
1. Pre-process LiDAR data:
   a. Filter data frames to remove background objects.
   b. Convert 3D point clouds into spherical coordinates.
   c. Cluster moving points to distinguish from background.
2. Extract and segment trajectories:
   a. Identify individual vehicle paths.
   b. Classify road users (vehicles, cyclists, pedestrians).
3. Prepare data for CNN:
   a. Represent vehicle states as input sequences (speed, direction, acceleration, proximity).
   b. Convert sequences into structured input matrices.
4. Define CNN architecture:
   a. Input layer to receive structured matrices.
   b. Convolutional layers to extract spatial and temporal features.
   c. Pooling layers to reduce dimensionality.
   d. Fully connected layers to interpret features and predict trajectories.
5. Train CNN model:
   a. Split data into training and validation sets.
   b. Train the CNN using training data.
   c. Validate the model using validation data and fine-tune hyperparameters.
6. Predict trajectories:
   a. Input current vehicle states into the trained CNN model.
   b. Estimate PET and TTC values for future time steps.
7. Evaluate and refine predictions:
   a. Compare predicted PET and TTC with actual values.
   b. Adjust model parameters to improve prediction accuracy.

Output: Predicted trajectories, PET, and TTC values

Extracting PET and TTC values from LiDAR sensor trajectories requires a detailed technical process. Initially, the trajectory data, capturing the movements of vehicles within the intersections, were pre-processed to identify individual vehicle paths. Subsequently, the PET and TTC values were computed based on the kinematic properties of each vehicle trajectory. PET was derived by evaluating the temporal and spatial gaps between vehicles along their paths. TTC was determined by assessing the time remaining before the projected intersection of vehicle paths occurred. Applying a CNN model, the trajectories were converted into structured input matrices or sequences. This involved representing the temporal evolution of vehicle states including speed, direction, acceleration, and proximity as a series of inputs. By training the CNN on these sequences, the network could recognize the complex patterns and relationships between the variables to estimate the PET and

TTC values. In other words, the network's convolutional layers employed learnable filters to extract spatial and temporal features. Through convolution and pooling operations, the network captured significant patterns, such as sudden changes in velocity, diverging directions, accelerating rates, and decreasing inter-vehicle distances. In terms of the vehicle trajectories obtained from the LiDAR sensors, subsequent data pre-processing was used encompasses trajectory extraction, segmentation, and classification, distinguishing vehicles, cyclists, and pedestrians to facilitate a nuanced analysis. The trajectory analysis provided in this paper focuses on several key metrics, including speed differentials, proximity events, and traffic density, to identify potential conflict areas for vehicle–vehicle and vehicle–pedestrian interactions. The following steps were taken into account to recognize the trajectories of vehicles and pedestrians:

1. In time intervals when no traffic passed from different approaches to the intersection, no traffic data frames were collected.
2. The LiDAR data frames were filtered to remove background objects identified from multiple no-traffic data frames.
3. The 3D point clouds were converted into spherical coordinates in order to create the elevation–azimuth matrix. A new data structure was created to store the range, azimuth, and intensity information from the raw LIDAR data.
4. Based on the reflectivity of the object and the wavelength of the LiDAR, a position packet and a data packet were created. GPS packets contain position information, while data packets contain distance and intensity information.
5. Moving points were clustered to make them easy to distinguish from the foreground and background. Azimuth–height tables were developed using azimuth–height background filtering. In different data frames, the height of each point was compared with the heights of the backgrounds to recognize and then classify road users and non-road users.

It is worth mentioning that PET and TTC values serve as valuable metrics for assessing collision risks at signalized intersections. However, integrating these metrics into traffic management and vehicle safety systems comes with inherent considerations. One of these significant considerations involves the reliance on predictive models, which may not encapsulate all real-world collision scenarios due to their basis on historical data and certain assumptions. Variability in driver behavior, unexpected events, and environmental conditions often challenge the accuracy of predictions based solely on PET and TTC values. Moreover, these metrics might overlook the context of individual driving styles, limitations in sensor accuracy, and uncertainties in vehicle movement predictions, leading to potential inaccuracies in collision risk assessment. To address these limitations, a multifaceted approach was utilized. This involved integrating the PET and TTC data with real-time information from multiple camera systems to capture a more comprehensive view of the surroundings. Hereupon, each intersection was monitored by closed-circuit television (CCTV) to capture a more comprehensive view of the surroundings. By utilizing advanced machine learning algorithms that consider real-time inputs, predictive capabilities were improved. The pseudocode for finding the PET and TTC values is explained in Appendix A.

Additionally, the models were validated with real-world collision data (crash data from 2018 to 2022) to improve their reliability and applicability within traffic management and vehicle safety systems. In order to investigate the accuracy of LiDAR sensor technology in recording V2V and V2P conflicts at signalized intersections, six different intersections in Trois-Rivières City, Quebec, Canada, were assessed. The LiDAR sensors were installed at all intersections simultaneously in January 2022 to record real-time traffic data, including vehicle and pedestrian counts, speeds, and vehicle–vehicle conflicts. The location of each intersection and the LiDAR sensors (the red circles) are shown in Figures 1–3, respectively. The red circles indicate the location of the LiDAR sensor's installation at each intersection.

Figure 1. Bd Saint-Jean and Boulevard Jean-XXⅠⅠⅠ Intersection (**left**)" and "RTE 138 and Rue Nicolas Parrot Intersection and one of LiDAR sensors (**right**).

Figure 2. Rue BELLEFEUILLE-Rue St-Roch St Intersection (**left**)" and "Rue BARKOFF and Rue des Ormeaux Intersection (**right**).

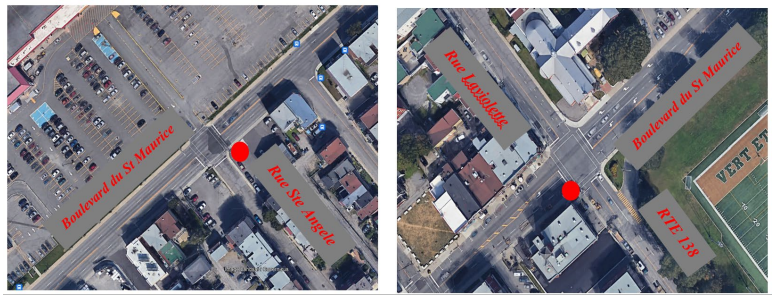

Figure 3. Boulevard du St Maurice-Rue Ste Angele Intersection (**left**)" and "Boulevard du St Maurice-Rue Laviolette Intersection (**right**).

The vehicle counts (including cars, trucks, and buses) and pedestrians over eighteen months were analyzed to determine the daily entering vehicle and pedestrian volumes at each intersection. These variables are utilized in the intersection crash rate equation. Additionally, the vehicle–vehicle conflicts based on leading and following vehicles, the direction of conflicts based on vehicles' trajectories, and the frequency and severity (=1/PET) of conflicts were analyzed. For the purpose of identifying the critical movements at each intersection based on the frequency and severity of conflicts, the conflicts with PET < 1 s [33] were analyzed. From 2018 to 2022, crash reports were analyzed to determine the exact locations of crashes at each intersection, the time of the day, the reason for the crash, and the severity of the crash (fatal, injury, and road/material damage) [34]. To determine the safety risk for each intersection, an intersection crash rate, as shown in Equation (1), was developed to describe the crashes per million entering vehicles to the intersection.

$$R = \frac{1,000,000 * C}{365 * N * V} \quad (1)$$

where,

R = Crash rate for the intersection expressed as crashes per million entering vehicles;
C = Total number of intersection crashes in the study period;

N = Number of years of data;
V = Traffic volumes entering the intersection daily.

The value of C was obtained from crash reports collected over the study period. It represents the total number of crashes that occurred at the intersection. The parameter N indicates the duration of the study period in years. This value ensures that the crash rate accounts for long-term trends and variations in crash occurrences. The parameter V represents the average daily traffic volume entering the intersection. These data are typically obtained from traffic counts or transportation models. To determine the crash rate, R, all other values were first extracted from crash reports and traffic volume data. Once these values were known, the crash rate was calculated using Equation (1). This calculated rate reflects the likelihood of crashes occurring per million vehicles entering the intersection, providing a clear and comparable measure of intersection safety. The threshold for setting crashes per million entering vehicles is based on safety performance standards and comparative analyses with similar intersections. By evaluating the crash rates across multiple intersections, thresholds can be established to identify intersections with significantly higher crash rates, warranting further investigation or intervention.

To determine the accuracy of LiDAR sensor technology, the critical movements detected by the LiDAR data analysis were compared with those identified in the crash reports. Critical movements refer to the leading or following movements that have a high frequency and severity of near-miss crashes or conflicts. This paper analyzed LiDAR data covering an 18-month period and compared them to a five-year investigation of intersection crash rates. Despite the discrepancy in data duration, the shorter LiDAR data collection did not result in an incomplete representation of intersection safety. Historical crash trends and patterns were examined to estimate and predict longer-term trends consistent with the five-year investigation period. This method ensures that the analysis provides a comprehensive and accurate assessment of intersection safety over both short- and long-term periods, by integrating real-time data with extensive historical records. LiDAR identified near-miss events and conflict points not captured in the crash data. Historical crash data offer context and a broader temporal perspective, helping to identify persistent safety issues and validate short-term observations. This combined approach enables a robust evaluation of safety measures and the development of effective intervention strategies, ensuring that findings are both current and historically grounded.

The historical crash trends and patterns were investigated to estimate and predict longer-term trends that aligned with the five-year investigation period. Furthermore, synthetic data were generated based on the patterns observed within the 18-month LiDAR dataset. Machine learning algorithms were employed to simulate the characteristics and trends observed in the original LiDAR dataset. By merging and cross-referencing multiple datasets (LiDAR and the historical crash data), a more comprehensive understanding of long-term intersection safety trends was achieved, so that the limitation of the shorter LiDAR data duration could be mitigated. To ensure the reliability and validity of the synthetic data, these synthetic data were compared against historical crash data to validate their accuracy, ensuring consistency in key metrics such as traffic volumes and conflict rates. Statistical analyses were performed to compare the distributions between the synthetic and original datasets, maintaining their statistical properties. Traffic simulations were run using the synthetic data, and the results were validated against real-world observations. These rigorous validation steps ensured that the synthetic data accurately represented long-term intersection safety trends, mitigating the limitations of the shorter LiDAR data duration and providing a robust foundation for comprehensive analysis.

The image-processing algorithm developed in MATLAB included the following steps: identifying vehicle boundaries in the LiDAR-generated point cloud data, identifying key features such as the corners and edges of vehicles, following the movements of identified vehicles across successive frames, and connecting the tracked positions over time to result in continuous paths representing the vehicles' movements. It is worth mentioning that the previous image-processing algorithm developed in MATLAB R2021b [2] was utilized to

analyze the vehicles' trajectories at six intersections. The MATLAB R2021b version was chosen for its advanced image-processing toolbox and computational efficiency, which were crucial for handling the large volume of LiDAR-generated data. The algorithm tailored for trajectory analysis utilized various image-processing techniques such as edge detection, feature extraction, and object tracking to interpret the LiDAR-generated point cloud data. This facilitated the extraction of vehicle trajectories by identifying and tracking individual vehicles' movements within the complex intersection environments. Leveraging MATLAB R2021b's capabilities allowed for efficient data processing, trajectory reconstruction, and subsequent analyses of key variables, including the speed, direction, and spatial interactions among vehicles. Although newer versions of MATLAB are available, R2021b was chosen to maintain consistency with previous work and because it had already been extensively tested and validated for similar tasks.

The research emphasizes the integration of intelligent transportation systems, particularly V2V and V2P communication technologies, to enhance safety measures. The methodology included field observations, traffic flow modeling, and scenario simulations to identify potential conflict points. Targeted interventions such as adaptive traffic signal control, enhanced crosswalk designs, and V2V communication protocols were developed based on the findings. This study underscores the role of sustainable transportation practices in increasing safety, optimizing traffic flow, and minimizing conflicts, aligning with the principles of sustainable transportation systems.

The identification of these conflict points can inform the development of targeted interventions, including adaptive traffic signal control, enhanced crosswalk designs, and the integration of V2V communication protocols. Furthermore, this study emphasizes the role of sustainable transportation practices in increasing the safety impact of vehicular travel. By optimizing traffic flow and minimizing conflicts, the proposed interventions align with the principles of sustainable transportation systems and promoting efficient resource use.

4. Results

Different conflict analyses were provided, including the monthly frequency, hourly frequency, hourly severity (sum 1/PET), and hourly average of the PETs. Figure 4 shows the monthly frequency, Figure 5 shows the hourly frequency, Figure 6 shows the hourly severity, and Figure 7 shows the hourly average of these PETs, respectively.

Figure 4 illustrates the monthly frequency of conflicts recorded at each of the six signalized intersections from January 2022 to June 2023. These conflicts, defined as potential near-misses between two vehicles, were identified and recorded using the LiDAR sensors installed at each intersection. The data collected by these sensors were accessible via a dedicated dashboard, allowing for detailed monitoring and analysis. The primary objective of presenting Figure 4 is to highlight the variations in conflict frequency over the specified period and across different intersections. This visualization is crucial for understanding the temporal patterns and potential factors contributing to traffic conflicts at these locations. The figure allows for the identification of trends, such as whether certain months or seasons exhibit higher conflict rates, which could be indicative of factors like changes in traffic volume, weather conditions, or the effectiveness of implemented traffic safety measures. By thoroughly analyzing the data presented in Figure 4, this study aims to inform traffic management strategies and enhance intersection safety.

As shown in Figure 5, the highest frequency of conflicts occurred in the interval 20:00–21:00 PM at intersections #1, #2, #5, and #6. The interval 12:00–13:00 PM (=13,941) at intersection #3 and the interval 18:00–19:00 PM (=10,453) at intersection #4 were specified as critical hourly intervals. The designation of the interval 18:00–19:00 PM as a critical hourly interval at intersection #4 was based on a comprehensive analysis of conflict frequency and traffic patterns. This interval recorded a significantly higher number of conflicts, totaling 10,453, compared to other times at the same intersection. Factors contributing to this designation included the high traffic volume and congestion during the evening rush hour,

increased pedestrian activity, and reduced visibility due to dusk or early evening darkness, especially in the winter months. Additionally, the specific geometric or operational characteristics of intersection #4, such as complex turning movements or inadequate signaling, may exacerbate conflict risks during this period. Historical data further validated this finding, showing a consistent pattern of increased incidents during the 18:00–19:00 PM interval over several years.

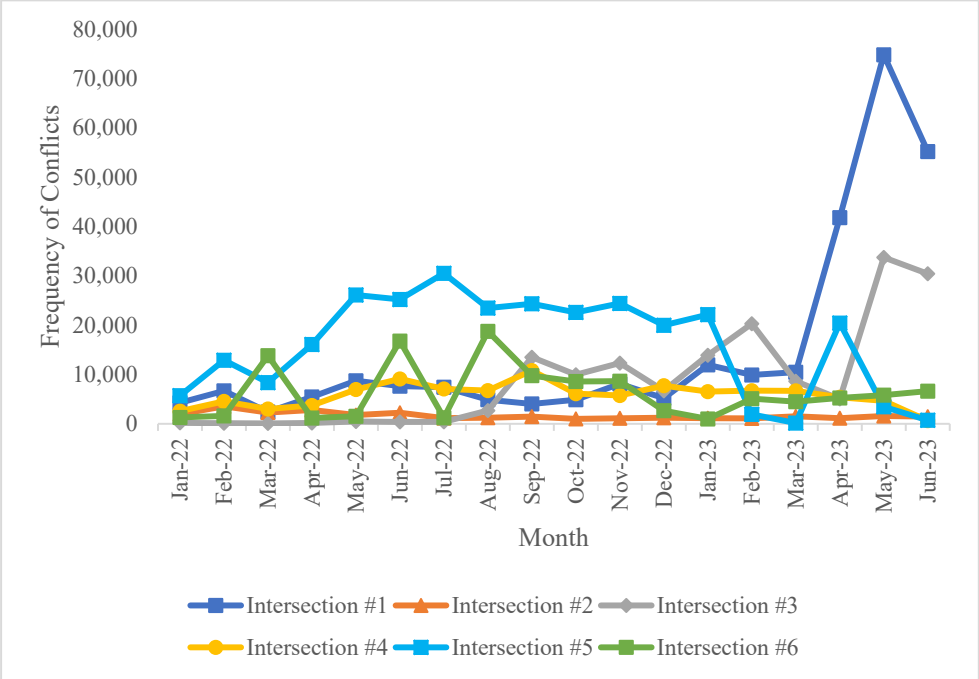

Figure 4. Monthly frequency of conflicts.

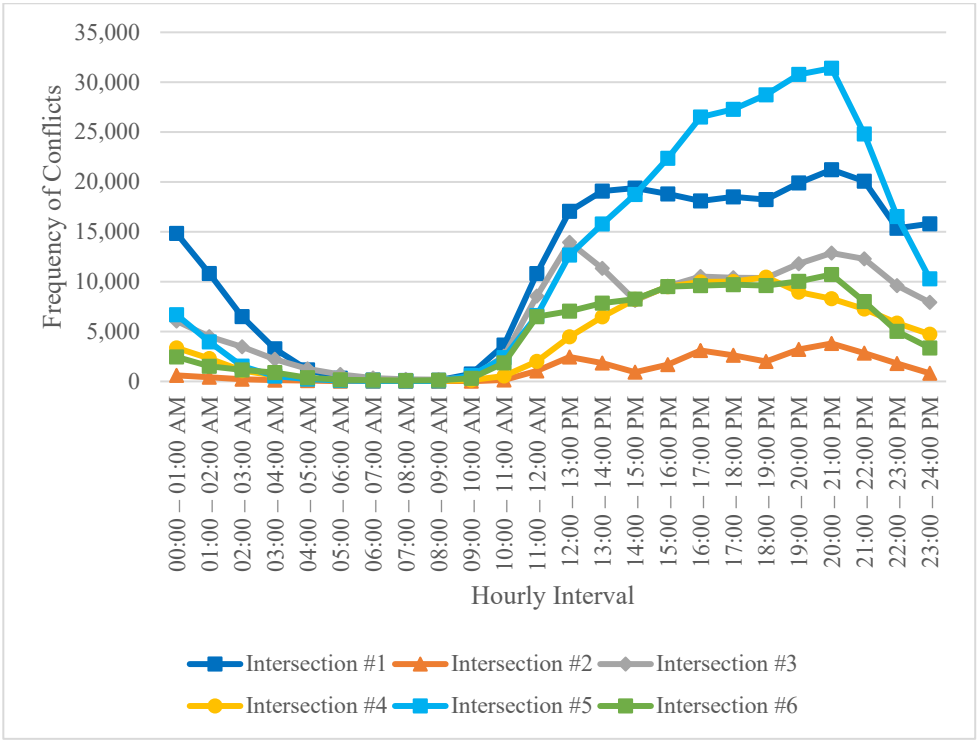

Figure 5. Hourly frequency of conflicts.

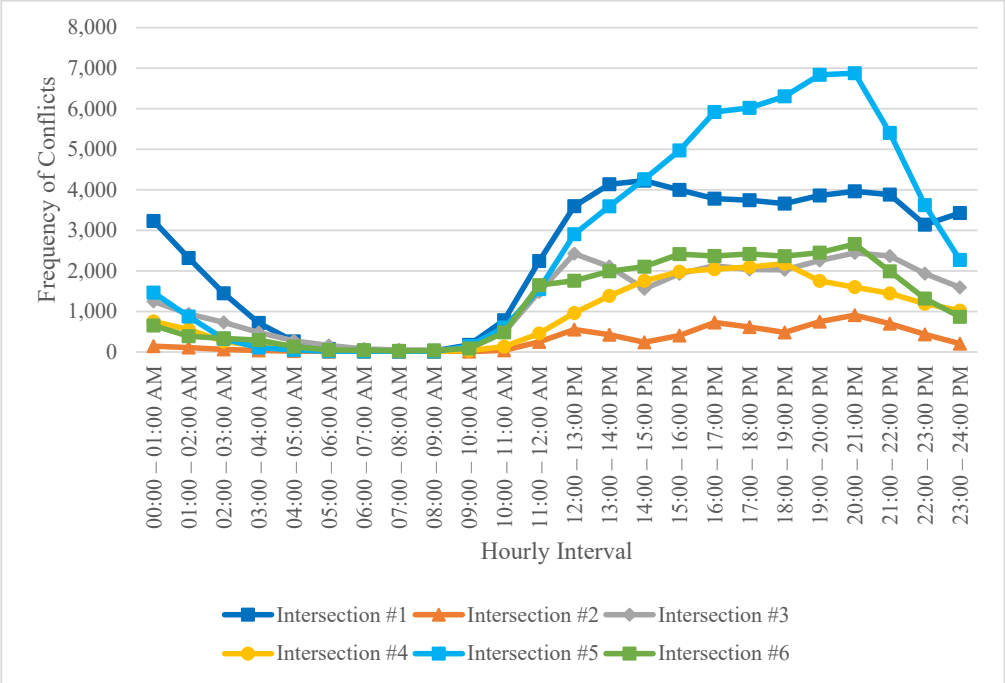

Figure 6. Hourly severity of conflicts.

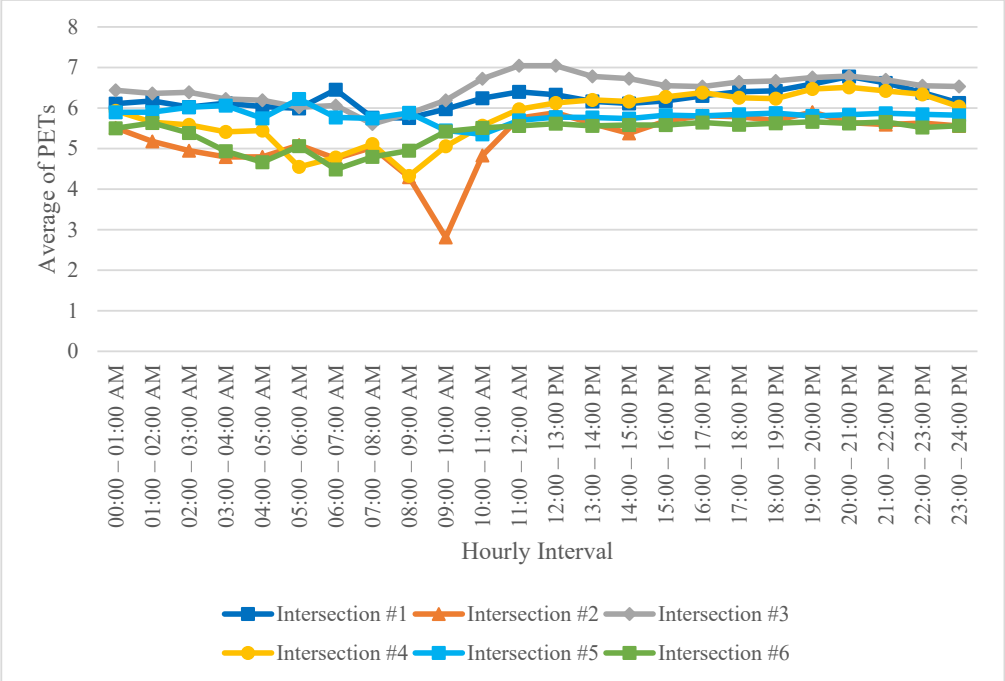

Figure 7. Hourly average PETs of the conflicts.

As shown in Figure 6, the interval 20:00–21:00 PM was specified as the interval with the most severe conflicts at intersections #2, #3, #5, and #6. Furthermore, the interval 14:00–15:00 PM at intersection #1 and 18:00–19:00 PM at intersection #4 were specified the hourly intervals with the most severe vehicle–vehicle conflicts, respectively. The averages of the PETs for each hourly interval are shown in Figure 7.

The frequency and severity of conflicts based on leading and following movements were analyzed for each intersection. At intersection #1, the movement WN (EBL—left turn from Boulevard Jean-XX|||| to Bd Saint-Jean) was specified as a frequent and severe leading movement. Additionally, the results of the following movements highlighted that

WN and EW (westbound through—WBT) were the movements with a greater frequency and severity of vehicle–vehicle conflicts. At intersection #2, the leading movement WN (EBL—left turn from RTE 138 to Rue Nicolas Parrot) and the following movement EW (WBT—through movement at RTE 138) were the movements with the highest frequency and severity of conflicts. At intersection #3, the leading movement NE (SBL—left turn from Rue BELLEFEUILLE to Rue St-Roch St) and the following movement SN (NBT—through movement at Rue BELLEFEUILLE) were frequent and severe vehicle–vehicle conflict movements. At intersection #4, the leading movement WN (EBL—left turn from Rue BARKOFF to Rue des Ormeaux St) and the following movement EW (WBT—through movement at Rue BARKOFF) were the movements with the highest frequency and severity of vehicle–vehicle conflicts. At intersection #5, the leading movement NE (SBL—left turn from the parking to Boulevard du St Maurice) and the following movement SN (NBT—through movement from Rue Ste Angele to parking) were the critical leading and following movements. Finally, at intersection #6, the leading and following movement EW (WBT—through movement at Boulevard du St Maurice) was the critical movement of the intersection #6.

To explore the vehicle–vehicle conflicts with the greatest potential for crashes (PET < 1 s) [33], movements including the origin and destination, frequency, severity ($1/\sum$PET), and average of TTC were analyzed. Table 1 demonstrates the critical near-crash movements observed at the six examined intersections.

Table 1. Near-crash conflicts analysis.

Intersection	Leading	Following	Frequency	Severity (1/PET)	Average TTC (s)	Total Conflicts (PET < 1 s)
Intersection #1	WN	EW	340	397.1	1.17	687
Intersection #2	WN	EW	87	97.3	0.78	316
Intersection #3	NE	SN	413	455.8	2.26	708
Intersection #4	WN	EW	72	79.6	1.36	628
Intersection #5	WN	EW	185	208.1	0.54	976
Intersection #6	EW	NA	560	690.9	1.52	1106

The tables presented in this section serve a critical role in analyzing the data underpinning our study, focusing on specific movements and traffic dynamics at various intersections. This analysis is essential for identifying high-risk movements, which is fundamental for devising targeted safety interventions. By summarizing and interpreting the data, the following tables highlight critical trends, validate findings with the crash data, and offer practical insights for improving traffic safety. The detailed examination provided here ensures that the research findings are robust and the implications for traffic management are clear and actionable. Moreover, Table 1 and Table 3 are directly related to the detailed tables in Appendix A, which offer in-depth details of the underlying data.

The results demonstrated in Table 1 are consistent with the results of Tables A1–A6 in the Appendix. According to Table A5, the leading movement NE and the following movement SN were identified as critical movements at intersection #5. The near-crash analysis demonstrated that movements WN and EW were more likely to lead to serious crashes. As specified in Table A5, the leading movement WN (=27,862 frequency) and the following movement EW (=29,837 frequency) were among the most frequent and severe movements in vehicle–vehicle conflicts.

To compare the accuracy of the data collected from the LiDAR sensors and the recorded crashes at each intersection over five years of investigation from police, insurance companies, and other reliable resources reports, the crash data of each intersection were downloaded [34] and analyzed accurately. The crash analysis results are demonstrated in Table 2.

Table 2. Crash reports analysis results.

Intersection #	Total Frequency of Crashes *	Type of Crash			Hourly Interval with the Highest Frequency of Crashes	Intersection Crash Rate (Equation (1)) **
		Fatal	Injury	Material/Road Damage		
#1	14	0	9	5	23:00–24:00 PM (3 crashes)	11.75
#2	4	0	3	1	08:00–09:00 AM (2 crashes)	7.02
#3	38	0	4	34	07:00–08:00 AM & 15:00–16:00 PM (5 crashes)	29.04
#4	34	2	9	23	16:00–17:00 PM (8 crashes)	17.91
#5	7	0	4	3	14:00–15:00 PM & 15:00–16:00 PM (2 crashes)	7.04
#6	34	0	12	22	16:00–17:00 PM (5 crashes)	28.88

* The frequency of recorded crashes by police, insurance companies, and other reliable resources. ** The values of this column show the number of crashes per million entering vehicles to the intersection.

Considering 653 veh/day, 312 veh/day, 717 veh/day, 1040 veh/day, 545 veh/day, and 645 veh/day entering intersections #1 to #6, respectively, the results highlighted that 11.75, 7.02, 29.04, 17.91, 7.04, and 28.88 crashes occurred per million entering vehicles to these six intersections. The trajectory of each crash at each intersection was analyzed, and the results revealed that 9 crashes at intersection #1 occurred with "WN-EW" leading and following movements, 3 crashes at intersection #2 occurred with "WN-EW" leading and following movements, 26 crashes at intersection #3 occurred with "NE-SN" leading and following movements, 24 crashes at intersection #4 occurred with "WN-EW" leading and following movements, 4 crashes at intersection #5 occurred with "WN-EW" leading and following movements, and 32 crashes at intersection #6 occurred with "EW" leading and following movements. Accordingly, the crash reports analysis yielded the same critical leading and following movements as shown in Table 2 based on the LiDAR sensor data. To assess the safety of pedestrians at the six intersections, the passing daily pedestrians were analyzed from the approaches where they interacted with these critical leading and following movements. Table 3 shows the normalized pedestrians who were at risk of being hit by critical leading and following movements. Considering the frequency of passing pedestrians at the critical approaches of each intersection, the highest calculated normalized pedestrian rates at risk of vehicle collisions were calculated for intersections #6, #4, and #3, respectively. Hereupon, safety considerations for the vehicles and pedestrians' movements should be implemented at these intersections.

Table 3. Normalized pedestrians who were at risk of being hit by vehicles.

Intersection #	Leading Vehicle Daily Volume (PCU/Day)	Following Vehicle Daily Volume (PCU/Day)	Critical Leading and Following Vehicle Movements	Total Daily Frequency of Pedestrians Who Are Interact with the Critical Leading and Following Vehicle Movements (People)	Normalized Pedestrian Rates at Risk of Vehicle Collisions
#1	100	112	WN-EW	22	0.103
#2	22	90	WN-EW	25	0.223
#3	72	109	NE-SN	92	0.508
#4	94	105	WN-EW	109	0.548
#5	63	95	WN-EW	34	0.215
#6	106		EW	116	1.094

The trajectory of each conflict at each intersection, the leading and following movements at each conflict, the intersections' gradients based on these leading and following movements, and the sight triangle at each conflict were analyzed. Considering our proposed vehicle–pedestrian conflict classification, including serious, general, slight, and potential conflicts [11], the lower and upper levels of each category were revised based on the physical characteristics of each intersection, the frequency and severity of conflicts, and the PET values. Hereupon, the new lower and upper levels are presented in Table 4.

Based on the findings presented in Table 4 and the conclusions drawn from this study, the following intervals are recommended for categorizing serious, general, slight, and potential conflicts at signalized intersections. These categories can be applied to other signalized intersections with similar physical and geometrical characteristics.

Serious Conflicts: PET < 0.9
General Conflicts: 0.9 ≤ PET <1.5
Slight Conflicts: 1.5 ≤ PET < 2.45
Potential Conflicts: 2.45 ≤ PET < 5

Table 4. PET Intervals for serious, general, slight, and potential conflicts.

Intersection #	Serious Conflicts	General Conflicts	Slight Conflicts	Potential Conflicts
#1	PET < 1.08	1.08 ≤ PET < 1.69	1.69 ≤ PET < 2.63	2.63 ≤ PET < 5
#2	PET < 0.99	0.99 ≤ PET < 1.6	1.6 ≤ PET < 2.54	2.54 ≤ PET < 5
#3	PET < 0.8	0.8 ≤ PET < 1.41	1.41 ≤ PET < 2.35	2.35 ≤ PET < 5
#4	PET < 0.78	0.78 ≤ PET < 1.39	1.39 ≤ PET < 2.33	2.33 ≤ PET < 5
#5	PET < 0.73	0.73 ≤ PET < 1.34	1.34 ≤ PET < 2.28	2.28 ≤ PET < 5
#6	PET < 1.02	1.02 ≤ PET < 1.63	1.63 ≤ PET < 2.57	2.57 ≤ PET < 5

Serious conflicts at signalized intersections represent scenarios with the highest risk of severe crashes and injuries. The recommended interval of PET < 0.9 for serious conflicts is justified by the critical nature of events falling within this range. These situations typically involve extremely short time gaps between conflicting movements, leaving little margin for error or evasive action by drivers. Such conditions are particularly prevalent in congested urban areas or at intersections with complex geometries, where traffic volumes and conflicting movements are high. By setting a threshold of PET < 0.9, it is possible to identify and prioritize interventions aimed at reducing the likelihood of catastrophic collisions. Potential measures may include signal phasing adjustments, geometric redesigns, or enhanced enforcement strategies to improve compliance with traffic regulations and enhance intersection safety.

General conflicts encompass scenarios where the risk of crashes at signalized intersections is elevated compared to normal operating conditions, but falls short of the severity observed in serious conflict situations. The interval of 0.9 ≤ PET < 1.5 for general conflicts strikes a balance between safety considerations and operational efficiency. Events falling within this range signify instances where the time gaps between conflicting movements are slightly longer, yet still pose a notable risk to traffic safety. Drivers may have limited time to react to changing traffic conditions, increasing the likelihood of rear-end or side-impact collisions. By identifying conflicts within this interval, it is possible to implement targeted measures such as signal timing adjustments, lane reconfigurations, or enhanced signage to mitigate risks and enhance intersection safety.

Slight conflicts denote situations where the risk of crashes at signalized intersections is moderate, with relatively longer time gaps between conflicting movements compared to serious and general conflict scenarios. The interval of 1.5 ≤ PET < 2.45 for slight conflicts reflects a nuanced understanding of intersection dynamics and the varying degrees of risk associated with different traffic scenarios. Events falling within this range indicate potential hazards that require attention but are less urgent compared to serious or general conflicts. Nonetheless, addressing conflicts within this interval is crucial for maintaining

overall intersection safety and preventing the escalation of minor to more severe crashes. Mitigation strategies may include targeted enforcement efforts, improved signal visibility, or enhanced driver education programs to promote safe driving behaviors and reduce the likelihood of collisions.

Potential conflicts represent situations where the risk of crashes at signalized intersections is relatively low, yet still warrants proactive monitoring and intervention. The interval of $2.45 \leq \text{PET} < 5$ for potential conflicts signifies scenarios with longer time gaps between conflicting movements, indicating a lower probability of immediate collisions. However, these events may still contribute to congestion, delays, or near-miss incidents, highlighting the need for ongoing surveillance and risk mitigation measures. It is possible to utilize data-driven approaches such as predictive modeling, intersection performance evaluations, or traffic simulation techniques to identify and address potential conflicts within this range. By implementing targeted interventions aimed at reducing minor incidents and optimizing traffic flow, agencies can enhance overall intersection safety and promote smoother traffic operations for all road users.

Considering the new lower and upper levels at each intersection, the frequency and severity of serious, general, slight, and potential conflicts were specified. Based on the new categories at each intersection, Table 5 shows the frequencies of serious, general, slight, and potential conflicts.

Table 5. The frequency results for serious, general, slight, and potential conflicts.

Intersection #	Serious Conflicts	General Conflicts	Slight Conflicts	Potential Conflicts	SUM
#1	1210	7509	20,158	245,102	273,979
#2	262	1008	2890	25,624	29,784
#3	42	3493	8087	147,500	159,122
#4	5	1776	6432	96,585	104,798
#5	1	3340	17,224	268,065	288,630
#6	1391	4666	13,744	94,411	114,212

Table 5 presents a comprehensive breakdown of the conflicts observed at different signalized intersections, categorized into four distinct levels: serious, general, slight, and potential conflicts. Each intersection is assigned a unique identifier, facilitating a comparison and analysis of conflict patterns across multiple locations. The table highlights the variability in conflict severity across different intersections, as evidenced by the varying distributions of conflicts in each category. For instance, intersections #1 and #5 exhibited a notably higher prevalence of potential conflicts compared to other categories, indicating a greater proportion of low-risk incidents relative to serious or general conflicts. In contrast, intersections #3 and #4 demonstrated a relatively higher incidence of slight and general conflicts, suggesting a moderate level of risk associated with these locations. This variability underscores the importance of context-specific analyses and targeted interventions tailored to address the unique challenges posed by each intersection. By quantifying the frequency of conflicts at each intersection, the hotspots with high concentrations of serious or potential conflicts, warranting immediate attention, were identified. Moreover, the distribution of conflicts across different severity levels enables a nuanced approach to resource allocation, ensuring that interventions are tailored to address the specific safety concerns at each location. For instance, intersections with a predominance of serious conflicts may require targeted engineering solutions such as geometric redesigns or signal phasing adjustments to mitigate risks effectively. Conversely, intersections with a higher incidence of general or slight conflicts may benefit from enforcement measures, signage enhancements, or driver education programs to promote safer behaviors and reduce the likelihood of crashes.

5. Discussion

This paper aimed to investigate how accurate LiDAR sensors are at detecting vehicle–vehicle conflicts at signalized intersections. Based on the PET values recorded by six LiDAR sensors at six different intersections of Trois-Rivières City, Quebec, Canada, the critical leading and following movements at each intersection were determined. To improve the accuracy of the analysis and compare it with recorded crash reports, data from 2018 to 2022 were analyzed. Table 2 shows that the critical movements from the crash reports aligned with those identified by LiDAR, confirming its effectiveness in recording near-crash vehicle–vehicle conflicts. The risk to pedestrians was assessed by examining the frequency of pedestrians passing through critical approaches and comparing it with vehicle volumes. Intersections #6, #4, and #3 had the highest vehicle–pedestrian conflict rates. To enhance safety and reduce conflicts, the following solutions are proposed:

Implementing advanced traffic signal systems with adaptive control can optimize signal timings based on real-time conditions, reducing congestion and potential conflicts [35]. Redesigning intersection geometries to improve visibility, increase turning radii, and minimize conflict points is essential, which may involve realigning or widening lanes [36]. Optimizing traffic signal timings through comprehensive studies and traffic simulation models can further reduce delays and queuing [37]. Integrating intelligent transportation systems, like vehicle-to-infrastructure communication, can provide real-time warnings and alerts to drivers about potential hazards [38]. Pedestrian safety can be improved by adding countdown signals, enhanced crosswalks, and refuge islands [39]. LiDAR technology provides real-time traffic data that can significantly improve traffic signal timing and coordination. By utilizing LiDAR to monitor and analyze traffic conditions continuously, it is possible to establish correlations between traffic flow patterns and signal phase distributions. These real-time data allow for dynamic adjustments to signal timings, reducing delays and mitigating bottlenecks at intersections. For example, LiDAR can help to optimize the duration of signal phases based on the current traffic volume and queue length, ensuring that each approach receives an adequate signal time proportional to its needs. This real-time adjustment capability will help to alleviate congestion and improve the overall traffic flow efficiency. Moreover, LiDAR's ability to communicate directly with traffic controllers and send/receive SPaT messages can enhance the synchronization of traffic signals across multiple intersections, further preventing bottlenecks and improving traffic management throughout the urban network [3–5]. Sensors mounted at intersections measure the numbers of vehicles, their speeds, and queue lengths, which are then used to dynamically adjust the durations of signal phases—green, yellow, and red.

Finally, the continuous monitoring and analysis of crash data at signalized intersections can identify high-risk areas and inform targeted interventions [40]. These combined approaches leverage advanced technologies and data-driven methods to ensure a comprehensive strategy for improving intersection safety.

The investigation conducted in this study highlighted the critical leading and following movements at each intersection. To validate the findings, crash reports spanning from 2018 to 2022 were examined from reliable sources such as police records and insurance companies. The results presented in Table 4 revealed a remarkable consistency between the critical movements identified through LiDAR datasets and those documented in crash reports. This alignment underscores the effectiveness of LiDAR sensors in efficiently capturing near-crash vehicle–vehicle conflicts, thereby affirming their utility in intersection safety assessments. Moreover, to gauge the risks posed to pedestrians by critical movements, the frequency of passing pedestrians from critical approaches was evaluated and compared with passing vehicle volumes. Subsequently, intersections #6, #4, and #3 emerged as hotspots with the highest rates of vehicle–pedestrian conflicts. These findings shed light on the pressing need to enhance pedestrian safety measures at these intersections in order to mitigate conflicts and reduce the likelihood of accidents. To address the identified challenges and enhance the safety of signalized intersections, several proactive solutions are proposed. Firstly, the implementation of advanced traffic signal systems, such as adap-

tive signal control, can optimize signal timings in response to real-time traffic conditions, thereby minimizing congestion and potential conflicts. Secondly, intersection geometry modifications, including realigning lanes and widening turning radii, can improve visibility and minimize points of conflict, contributing to overall intersection safety. Additionally, traffic signal timing optimization through comprehensive studies and data-driven approaches can alleviate delays, queuing, and conflicts. Integrating intelligent transportation systems, such as vehicle-to-infrastructure communication, can provide real-time warnings to drivers about potential conflicts or hazards, enhancing safety. Furthermore, implementing pedestrian safety measures like countdown signals and crosswalk enhancements can mitigate conflicts between vehicles and pedestrians, thereby improving overall intersection safety. Continuous data analysis and monitoring of crash data at signalized intersections are also recommended to identify high-risk areas and trends requiring targeted interventions. By implementing these multifaceted solutions, transportation agencies can work towards minimizing vehicle–vehicle and vehicle–pedestrian conflicts, thereby enhancing intersection safety and promoting smoother traffic flow for all road users.

6. Conclusions

This paper aimed to compare the accuracy of LiDAR sensor technology with traditional crash reports to recognize critical movements and decrease vehicle–vehicle conflicts at signalized intersections. From January 2022 to June 2023, the study examined datasets of the vehicle–vehicle conflicts at six distinct intersections in Trois-Rivières City, Quebec, Canada. The study focused on the recorded data from six LiDAR sensors, as shown in Appendix A, providing insights into the conflicts that occurred during the specified period. Through the examination of the conflict trajectories at each intersection and the identification of the PET and TTC values for leading and following movements, the crucial leading and following movements were identified. As shown in Table 1, "WN–EW (=EBL and WBT)" were recognized as the critical leading and following movements for intersections #1, #2, #4, and #5. At intersection #3, the leading movement NE (=SBL) and the following movement SN (=NBT) were identified as crucial movements. At intersection #6, the movement EW (=WBT) was recognized as the critical leading and following movement, resulting in 560 near-crash conflicts with PET < 1 s.

To enhance the accuracy of the analysis, the crash record datasets of the six intersections from 2018 to 2022 were analyzed. Investigating crash report analyses from reliable sources offers several benefits. Firstly, it helps in identifying the patterns and trends of crashes, aiding in understanding the common causes and contributing factors. This information can then be used to implement effective safety measures and improve traffic management strategies. Secondly, analyzing crash reports provides valuable insights into the severity and types of injuries sustained, assisting in prioritizing areas that require immediate attention. Lastly, it enables policymakers and authorities to make informed decisions regarding infrastructure improvements and targeted enforcement efforts to reduce crashes and enhance overall road safety. The crash report analysis revealed that 9 crashes at intersection #1 were caused by "WN–EW" leading and following movements, 3 crashes at intersection #2 by "WN–EW" movements, 26 crashes at intersection #3 by "NE–SN" movements, 24 crashes at intersection #4 by "WN–EW" movements, 4 crashes at intersection #5 by "WN–EW" movements, and 32 crashes at intersection #6 by "EW" movements.

The analysis of crash reports and LiDAR sensor data confirmed similar critical leading and following movements, as presented in Table 1. Consequently, the intersections' crash rates were calculated based on the daily entering vehicle counts and the frequency of recorded crashes over the five-year period. As shown in Table 2, intersections #3, #6, #4, #1, #5, and #2, respectively, require prioritized safety interventions based on their crash rates. Table 3 identifies the intersections with the highest potential for pedestrian conflicts with critical leading and following vehicles. The new vehicle–pedestrian categories depicted in Table 4 classify these vehicle–pedestrian conflicts into four categories: serious, general,

slight, and potential. The frequencies of vehicle–pedestrian conflicts at each intersection, as demonstrated in Table 5, were determined using these new categories.

In conclusion, this research demonstrates that the adoption of LiDAR sensor technology, in conjunction with traditional crash reports, can significantly enhance the understanding and management of vehicle–vehicle and vehicle–pedestrian conflicts at signalized intersections. The key benefits of this approach include the ability to capture real-time, high-resolution data on vehicle and pedestrian movements, speeds, and proximity, which traditional crash reports cannot provide.

The main contributions of this research include the identification of the critical leading and following movements at specific intersections, the validation of LiDAR data through a comparative analysis with traditional crash reports, and the development of new categories for vehicle–pedestrian conflicts. These findings offer a robust framework for future studies and practical applications, helping to prioritize safety interventions and infrastructure improvements. Other scholars can build on this research by integrating LiDAR sensor data with advanced analytics and machine learning models, such as Support Vector Machines (SVMs), Random Forests, Convolutional Neural Networks (CNNs), and Recurrent Neural Networks (RNNs). These models can be trained on labeled datasets of vehicle–vehicle conflicts to identify patterns and predict potential conflicts more accurately. Future research should also explore expanding the time interval and improving access to more reliable crash report sources to enhance the robustness of the findings.

Author Contributions: For this research article, A.A. contributed to conceptualization, methodology, formal analysis, investigation, resources, data curation, writing—original draft preparation, visualization, and project administration. M.J. contributed to validation, investigation, writing—review and editing, visualization, and supervision. All authors have read and agreed to the published version of the manuscript.

Funding: This research received no external funding.

Institutional Review Board Statement: Ethical review and approval were not required for this study.

Informed Consent Statement: Not applicable.

Data Availability Statement: The data used in this paper are real-time processed LiDAR data, which can be shared with the editorial board. The data utilized in this paper originates from LiDAR sensor dashboards, and along with freely accessible crash report datasets provided by the Quebec government website. The authors confirm the accuracy and availability of the datasets.

Acknowledgments: This study was supported by the SMARTER Centre, a Tier 1 University Transportation Centre of the U.S. Department of Transportation University Transportation Centers Program at Morgan State University.

Conflicts of Interest: The authors declare no conflicts of interest.

Appendix A

The purpose of Tables A1–A6 is to present the underlying data used to highlight the critical movements and understand the unique traffic dynamics at each intersection. These data are essential for developing effective safety interventions by targeting the movements with the highest risk. These detailed tables support the main findings by summarizing the data to identify and prioritize critical movements, corroborate them with the crash data, and provide actionable insights for traffic safety improvements. By providing this detailed introduction and interpretation of Tables A1–A6, the aim is to ensure that the concepts are self-contained and easily understood by the readers.

Table A1. Intersection #1's conflict data analysis.

	Leading Movements				Following Movements		
	Frequency	**Average PET**	**Severity**		**Frequency**	**Average PET**	**Severity**
EE (U-TURN)	521	4.822	200.2	EE (U-TURN)	495	5.177	147.2
EN	2783	6.01	610.2	EN	2261	5.951	532.2
EW	98,704	6.57	18,161.8	EW	121,940	5.884	28,715.7
NE	55,139	6.99	9954.9	NE	22,168	6.388	4672.9
NN (U-TURN)	914	5.909	217.5	NN (U-TURN)	620	6.097	141.0
NS	892	6.066	189.7	NS	821	5.417	208.6
NW	2778	6.047	623.8	NW	2575	5.7	663.0
SN	6	4.65	1.4	SN	6	3.75	2.2
SS (U-TURN)	8	7.83	1.0	SS (U-TURN)	5	6.68	0.9
SW	616	5.63	146.8	SW	983	6.777	176.9
WE	767	6.16	167.7	WE	526	5.585	137.7
WN	107,755	5.84	25,713.9	WN	118,529	6.83	20,740.5
WS	50	6.18	10.5	WS	33	6.448	6.2
WW (U-TURN)	482	6.147	108.1	WW (U-TURN)	354	6.656	63.3

Table A2. Intersection #2's conflict data analysis.

	Leading Movements				Following Movements		
	Frequency	**Average PET**	**Severity**		**Frequency**	**Average PET**	**Severity**
EE (U-TURN)	101	5.623	25.46	EE (U-TURN)	72	6.078	16.71
EN	52	6.252	10.12	EN	44	6.0235	9.72
EW	2708	6.523	532.76	EW	12643	5.217	3253.9
ES	6702	5.871	1516.2	ES	1676	5.591	409.3
NE	876	5.718	194.1	NE	1298	6.983	213.68
NS	95	6.385	17.21	NS	379	7.213	60.24
NW	22	6.053	5.14	NW	27	5.66	7.148
SN	343	6.561	61.91	SN	984	6.494	191.4
SE	363	6.084	74.77	SE	278	6.068	64.21
SS (U-TURN)	27	6.221	6.19	SS (U-TURN)	35	6.7	6.11
SW	375	6.143	79.6	SW	850	6.573	157.51
WE	4259	6.253	949.57	WE	7932	5.803	1909.61
WN	11,104	5.174	2888.1	WN	749	5.182	206.8
WS	30	6.52	6.69	WS	43	6.15	9.36
WW (U-TURN)	11	5.19	2.67	WW (U-TURN)	2	9.0425	0.22

Table A3. Intersection #3's conflict data analysis.

	Leading Movements				Following Movements		
	Frequency	**Average PET**	**Severity**		**Frequency**	**Average PET**	**Severity**
EE (U-TURN)	203	5.68	46.51	EE (U-TURN)	266	6.632	52.46
EN	50	5.898	12.94	EN	60	5.958	13.49
EW	40	5.904	9.22	EW	51	6.316	9.80
ES	28	5.266	6.77	ES	23	5.754	4.99
NE	45,676	5.527	11937.51	NE	12,216	6.22	2533.7
NN (U-TURN)	286	6.243	59.28	NN (U-TURN)	220	6.525	43.82
NS	21,731	7.075	3459.65	NS	18,907	7.821	2691.61
NW	90	6.082	19.6	NW	89	6.596	16.95
SN	31,543	6.697	5663.58	SN	67,653	6.266	15194.2
SE	857	6.002	182.8	SE	559	5.519	143.31
SS (U-TURN)	34	5.28	8.46	SS (U-TURN)	47	5.962	10.13
SW	269	5.195	72.47	SW	101	6.182	19.37
WE	30,502	7.972	4159.07	WE	26,024	7.216	4091.27
WN	14,860	7.751	2185.96	WN	20,517	6.844	3523.82
WS	1306	5.666	312.52	WS	1137	5.528	288.5
WW (U-TURN)	129	5.997	27.85	WW (U-TURN)	165	6.247	35.44

Table A4. Intersection #4's conflict data analysis.

	Leading Movements				Following Movements		
	Frequency	**Average PET**	**Severity**		**Frequency**	**Average PET**	**Severity**
EE (U-TURN)	34	4.723	10.17	EE (U-TURN)	23	6.023	4.705
EN	1239	5.967	247.63	EN	472	5.578	119.83
EW	6021	5.927	1374.9	EW	18,910	6.088	4092.2
ES	2469	5.362	652.93	ES	12,052	6.782	2177.3
NE	1728	6.308	348.66	NE	1443	5.589	347.06
NN (U-Turn)	48	6.004	10.32	NN (U-Turn)	54	5.37	13.71
NS	5065	6.838	906.13	NS	3352	6.36	677.73
NW	9892	6.158	1919.1	NW	7737	5.682	1853.31
SN	12,416	6.697	2287.2	SN	4954	5.583	1252.3
SE	2316	5.9	512.56	SE	1838	5.176	557.31
SS (U-TURN)	23	7.104	3.71	SS (U-TURN)	36	5.888	8.447
SW	12,569	7.38	1989.8	SW	5936	6.406	1241.44
WE	4833	5.885	1136.3	WE	4299	5.448	1119.48
WN	20,942	6.133	4479.5	WN	16,854	6.822	3140.55
WS	1665	6.25	335.12	WS	1644	5.562	412.81
WW (U-TURN)	66	5.636	16.56	WW (U-TURN)	62	5.9125	13.6

Table A5. Intersection #5's conflict data analysis.

	Leading Movements				Following Movements		
	Frequency	**Average PET**	**Severity**		**Frequency**	**Average PET**	**Severity**
EE (U-TURN)	176	5.632	42.93	EE (U-TURN)	167	5.844	35.38
EN	13,910	5.958	3061.1	EN	12,861	5.907	2788.25
EW	37,867	6.632	7030.4	EW	29,837	5.641	7353
ES	323	5.774	78.61	ES	182	5.821	39.31
NE	66,196	5.08	16746	NE	46,303	5.975	9885.34
NN (U-TURN)	222	5.792	46.76	NN (U-TURN)	279	5.584	63.71
NS	318	6.155	65.03	NS	592	6.425	113.18
NW	28,871	5.928	5977.9	NW	25,662	5.637	6279.18
SN	22,837	5.545	5401.3	SN	62,874	5.102	15,930.68
SE	3054	6.02	627.93	SE	2938	5.81	662.36
SS (U-TURN)	265	5.536	65.12	SS (U-TURN)	280	5.853	62.56
SW	14,119	6.332	2670.8	SW	18,319	5.999	3897.25
WE	18,840	6.594	3481.9	WE	5930	6.078	1314.8
WN	27,862	5.662	6797.3	WN	13,801	6.302	2842.42
WS	66	5.592	15.38	WS	49	6.0138	10.73
WW (U-TURN)	76	5.451	18.49	WW (U-TURN)	49	6.14	10.18

Table A6. Intersection #6's conflict data analysis.

	Leading Movements				Following Movements		
	Frequency	**Average PET**	**Severity**		**Frequency**	**Average PET**	**Severity**
EE (U-TURN)	85	4.45	27.12	EE (U-TURN)	51	5.526	12.23
EN	930	5.438	237.14	EN	659	5.882	149.03
EW	40,955	5.701	9958.3	EW	36,385	5.463	9704.55
ES	2793	5.675	679.93	ES	5225	6.508	486.66
NN (U-TURN)	7	6.112	1.302	NN (U-TURN)	10	7.24	1.77
NE	20,386	5.383	5144	NE	25,404	5.95	5756.7
NS	3033	5.882	681.52	NS	2946	5.346	761.8
NW	1881	5.324	537.08	NW	4003	4.49	1426.08
SN	4045	5.88	885.5	SN	7786	4.915	2165.26
SE	66	5.55	18.55	SE	102	4.535	31.16
SS (U-TURN)	4	5.497	0.86	SS (U-TURN)	7	6.027	1.33
SW	4034	6.252	837.1	SW	2489	4.766	771.7
WE	4599	5.761	1091	WE	6146	6.277	1266.68
WN	18,890	6.026	4276.4	WN	19,162	5.746	4398.2
WS	39	4.27	13.66	WS	40	5.2421	10.48
WW (U-TURN)	463	4.682	154.68	WW (U-TURN)	157	4.695	57.42

Pseudo code of PET and TTC Calculation:
# Step 1: Pre-process LiDAR Data
# Input: LiDAR data frames capturing vehicle and pedestrian movements
# Output: Filtered point cloud data with background objects removed
# 1.1 Filter data frames to remove background objects
for each frame in LiDAR data:
if no traffic in frame:
$P_{\text{background}}$ = frame
else:
P_{filtered} = frame $- P_{\text{background}}$
# 1.2 Convert 3D point clouds into spherical coordinates
for each point (x, y, z) in P_{filtered}:
r = sqrt($x^2 + y^2 + z^2$)
theta = atan2(y, x)
phi = acos(z/r)
spherical points.append((r, theta, phi))
# Step 2: Extract and Segment Trajectories
# Output: Identified and classified trajectories for vehicles and pedestrians
# 2.1 Cluster moving points to distinguish from background using DBSCAN
epsilon = 0.5 # Threshold distance for clustering
$min_{samples}$ = 5 # Minimum number of points to form a cluster
clusters = DBSCAN (eps = epsilon, $min_{samples}$ = $min_{samples}$).fit(spherical_points)
# 2.2 Identify and classify road users (vehicles, cyclists, pedestrians)
for each cluster in clusters:
height$_{diff}$ = abs (cluster.z $-$ background$_{height}$)
if height$_{diff}$ <= $height_{\text{threshold}}$:
if velocity(cluster) > $vehicle_{\text{threshold}}$:
vehicles.append(cluster)
else:
pedestrians.append(cluster)
# Step 3: Prepare Data for CNN
# Output: Structured input matrices representing vehicle states
# 3.1 Represent vehicle states as input sequences (speed, direction, acceleration, proximity)
for each vehicle in vehicles:
state$_{sequence}$ = (vehicle.speed, vehicle.direction, vehicle.acceleration, vehicle.proximity)
Input sequences.append(state sequence)
3.2 Convert sequences into structured input matrices
Structured matrices = reshape(input sequences)
Step 4: Define and Train CNN Model
Output: Trained CNN model for predicting trajectories
4.1 Define CNN architecture
Cnn model = Sequential()
Cnn model.add (Conv2D(filters = 32, kernel size = (3, 3), activation = 'relu', input shape = input shape))
Cnn model.add (MaxPooling2D(pool size = (2, 2)))
Cnn model.add (Flatten())
Cnn model.add (Dense(128, activation = 'relu'))
Cnn model.add (Dense(num classes, activation = 'softmax'))
4.2 Train the CNN using training data
Cnn model.compile (optimizer = 'adam', loss = 'categorical crossentropy', metrics = ['accuracy'])
Cnn model.fit (training data, training labels, validation data = (validation data, validation labels), epochs = 10)
Step 5: Predict Trajectories and Calculate PET and TTC

Output: Predicted trajectories, PET, and TTC values
5.1 Input current vehicle states into the trained CNN model to predict future trajectories
$Predicted_{\text{trajectories}}$ = cnn model.predict (structured_matrices)
# 5.2 Calculate PET and TTC values
for each trajectory in $Predicted_{\text{trajectories}}$:
for each $time_{step}$ in trajectory:
# Calculate PET
$t_{first} = time_{step}$ [0]
$t_{second} = time_{step}$ [1]
PET = $t_{second} - t_{first}$
# Calculate TTC
d_{initial} = sqrt $((\text{x1} - \text{x2})^2 + (\text{y1} - \text{y2})^2)$
v_{relative} = sqrt $((vx1 - vx2)^2 + (vy1 - vy2)^2)$
TTC = initial/v_{relative}
# Step 6: Evaluate and Refine Predictions
# Output: Refined PET and TTC values with improved accuracy
# 6.1 Compare predicted PET and TTC with actual values
for each actual value, predicted value in zip (actual data, predicted data):
error = abs(actual value – predicted value)
if error > tolerance:
adjust model parameters()
Return: Final predicted trajectories, PET, and TTC values
return predicted trajectories, PET, TTC

References

1. Anisha, A.M.; Abdel-Aty, M.; Abdelraouf, A.; Islam, Z.; Zheng, O. Automated Vehicle to Vehicle Conflict Analysis at Signalized Intersections by Camera and LiDAR Sensor Fusion. *Transp. Res. Rec.* **2023**, *2677*, 117–132. [CrossRef]
2. Ansariyar, A.; Jeihani, M. Investigating the Vehicle-Bicyclists Conflicts using LIDAR sensor technology at signalized intersections. In Proceedings of the ICTTE 2023: International Conference on Transportation and Traffic Engineering, Wuhan, China, 29–31 December 2023. [CrossRef]
3. Retallack, A.E.; Ostendorf, B. Current Understanding of the Effects of Congestion on Traffic Accidents. *Int. J. Environ. Res. Public Health* **2019**, *16*, 3400. [CrossRef] [PubMed]
4. Ansariyar, A.; Taherpour, A. Statistical analysis of vehicle-vehicle conflicts with a LIDAR sensor in a signalized intersection. *Adv. Transp. Stud.* **2023**, *60*, 4246. [CrossRef]
5. Wang, X.; Abdel-Aty, M. Temporal and spatial analyses of rear-end crashes at signalized intersections. *Accid. Anal. Prev.* **2006**, *38*, 1137–1150. [CrossRef] [PubMed]
6. Shinar, D. Crash causes, countermeasures, and safety policy implications. *Accid. Anal. Prev.* **2019**, *125*, 224–231. [CrossRef] [PubMed]
7. Retting, R.A.; Williams, A.F.; Preusser, D.F.; Weinstein, H.B. Classifying urban crashes for countermeasure development. *Accid. Anal. Prev.* **1995**, *27*, 283–294. [CrossRef] [PubMed]
8. Ansariyar, A.; Taherpour, A. Investigating the accuracy rate of vehicle-vehicle conflicts by LIDAR technology and microsimulation in VISSIM and AIMSUN. *Adv. Transp. Stud.* **2023**, *61*, 37–52.
9. Wu, J.; Xu, H.; Zheng, Y.; Tian, Z. A novel method of vehicle-pedestrian near-crash identification with roadside LiDAR data. *Accid. Anal. Prev.* **2018**, *121*, 238–249. [CrossRef] [PubMed]
10. Huang, X.; He, P.; Rangarajan, A.; Ranka, S. Intelligent Intersection: Two-stream convolutional networks for real-time near-accident detection in traffic video. *ACM Trans. Spat. Algorithms Syst.* **2020**, *6*, 1–28. [CrossRef]
11. Ansariyar, A.; Ardeshiri, A.; Jeihani, M. Investigating the collected vehicle-pedestrian conflicts by a LIDAR sensor based on a new Post Encroachment Time Threshold (PET) classification at signalized intersections. *Adv. Transp. Stud.* **2023**, *61*, 103–118.
12. Essa, M.; Sayed, T. Traffic conflict models to evaluate the safety of signalized intersections at the cycle level. *Transp. Res. Part C Emerg. Technol.* **2018**, *89*, 289–302. [CrossRef]
13. Kabil, A.; Rabieh, K.; Kaleem, F.; Azer, M.A. Vehicle to Pedestrian Systems: Survey, Challenges and Recent Trends. *IEEE Access* **2022**, *10*, 123981–123994. [CrossRef]
14. Sewalkar, P.; Seitz, J. Vehicle-to-Pedestrian Communication for Vulnerable Road Users: Survey, Design Considerations, and Challenges. *Sensors* **2019**, *19*, 358. [CrossRef] [PubMed]
15. Zheng, L.; Ismail, K.; Meng, X. Traffic conflict techniques for road safety analysis: Open questions and some insights. *Can. J. Civ. Eng.* **2014**, *41*, 633–641. [CrossRef]

16. Katrakazas, C.; Quddus, M.; Chen, W.-H. A Simulation Study of Predicting Real-Time Conflict-Prone Traffic Conditions. *IEEE Trans. Intell. Transp. Syst.* **2017**, *19*, 3196–3207. [CrossRef]
17. Gholamhosseinian, A.; Seitz, J. A Comprehensive Survey on Cooperative Intersection Management for Heterogeneous Connected Vehicles. *IEEE Access* **2022**, *10*, 7937–7972. [CrossRef]
18. Yuan, C.; Li, Y.; Huang, H.; Wang, S.; Sun, Z.; Li, Y. Using traffic flow characteristics to predict real-time conflict risk: A novel method for trajectory data analysis. *Anal. Methods Accid. Res.* **2022**, *35*, 100217. [CrossRef]
19. Xu, H.; Tian, Z.; Wu, J.; Liu, H.; Zhao, J. *High-Resolution Micro Traffic Data from Roadside LiDAR Sensors for Connected-Vehicles and New Traffic Applications*; No. P224-14-803 TO15; University of Nevada, Solaris University Transportation Center, High-Resolution Micro Traffic Data from Roadside LiDAR Sensors for Connected-Vehicles and New Traffic Applications: Reno, NV, USA, 2018.
20. Sohail, A.; Cheema, M.A.; Ali, M.E.; Toosi, A.N.; Rakha, H.A. Data-driven approaches for road safety: A comprehensive systematic literature review. *Saf. Sci.* **2023**, *158*, 105949. [CrossRef]
21. Bhattarai, N.; Zhang, Y.; Liu, H.; Pakzad, Y.; Xu, H. Proactive Safety Analysis Using Roadside LiDAR Based Vehicle Trajectory Data: A Study of Rear-End Crashes. *Transp. Res. Rec.* **2024**, *2678*, 772–785. [CrossRef]
22. Olugbade, S.; Ojo, S.; Imoize, A.L.; Isabona, J.; Alaba, M.O. A Review of Artificial Intelligence and Machine Learning for Incident Detectors in Road Transport Systems. *Math. Comput. Appl.* **2022**, *27*, 77. [CrossRef]
23. Li, F.; Yigitcanlar, T.; Nepal, M.; Nguyen, K.; Dur, F. Machine learning and remote sensing integration for leveraging urban sustainability: A review and framework. *Sustain. Cities Soc.* **2023**, *96*, 104653. [CrossRef]
24. Cooper, P. Experience with traffic conflicts in Canada with emphasis on "post encroachment time" techniques. In *International Calibration Study of Traffic Conflict Techniques*; Springer: Berlin/Heidelberg, Germany, 1984; pp. 75–96. [CrossRef]
25. Lee, D.N. A Theory of Visual Control of Braking Based on Information about Time-to-Collision. *Perception* **1976**, *5*, 437–459. [CrossRef] [PubMed]
26. Hoffmann, E.R.; Mortimer, R.G. Drivers' estimates of time to collision. *Accid. Anal. Prev.* **1994**, *26*, 511–520. [CrossRef] [PubMed]
27. Minderhoud, M.M.; Bovy, P.H. Extended time-to-collision measures for road traffic safety assessment. *Accid. Anal. Prev.* **2001**, *33*, 89–97. [CrossRef] [PubMed]
28. Cavallo, V.; Laurent, M. Visual Information and Skill Level in Time-To-Collision Estimation. *Perception* **1988**, *17*, 623–632. [CrossRef] [PubMed]
29. Bosnak, M.; Skrjanc, I. Efficient Time-To-Collision Estimation for a Braking Supervision System with LIDAR. In Proceedings of the 2017 3rd IEEE International Conference on Cybernetics (CYBCONF), Exeter, UK, 21–23 June 2017; pp. 1–6.
30. Jang, J.-A.; Choi, K.; Cho, H. A Fixed Sensor-Based Intersection Collision Warning System in Vulnerable Line-of-Sight and/or Traffic-Violation-Prone Environment. *IEEE Trans. Intell. Transp. Syst.* **2012**, *13*, 1880–1890. [CrossRef]
31. Das, S.; Maurya, A.K. Defining Time-to-Collision Thresholds by the Type of Lead Vehicle in Non-Lane-Based Traffic Environments. *IEEE Trans. Intell. Transp. Syst.* **2019**, *21*, 4972–4982. [CrossRef]
32. Saffarzadeh, M.; Nadimi, N.; Naseralavi, S.; Mamdoohi, A.R. A general formulation for time-to-collision safety indicator. In *Proceedings of the Institution of Civil Engineers-Transport*; Thomas Telford Ltd.: London, UK, 2013. [CrossRef]
33. Hydén, C. Traffic conflicts technique: State-of-the-art. *Traffic Saf. Work. Video Process.* **1996**, *37*, 3–14.
34. Quebec, G.O. Quebec Open Data Portal. 2023. Available online: https://www.donneesquebec.ca/ (accessed on 1 December 2020).
35. Hu, L.; Ou, J.; Huang, J.; Chen, Y.; Cao, D. A Review of Research on Traffic Conflicts Based on Intelligent Vehicles. *IEEE Access* **2020**, *8*, 24471–24483. [CrossRef]
36. Aryal, P. Optimization of Geometric Road Design for Autonomous Vehicle. 2020. Available online: http://www.diva-portal.org/smash/record.jsf?pid=diva2:1527750&dswid=-5140 (accessed on 1 December 2020).
37. Qadri, S.S.S.M.; Gökçe, M.A.; Öner, E. State-of-art review of traffic signal control methods: Challenges and opportunities. *Eur. Transp. Res. Rev.* **2020**, *12*, 1–23. [CrossRef]
38. Creß, C.; Bing, Z.; Knoll, A.C. Intelligent Transportation Systems Using Roadside Infrastructure: A Literature Survey. *IEEE Trans. Intell. Transp. Syst.* **2023**, *25*, 6309–6327. [CrossRef]
39. Li, Y.; Fernie, G. Pedestrian behavior and safety on a two-stage crossing with a center refuge island and the effect of winter weather on pedestrian compliance rate. *Accid. Anal. Prev.* **2010**, *42*, 1156–1163. [CrossRef] [PubMed]
40. Cheng, Z.; Zu, Z.; Lu, J. Traffic Crash Evolution Characteristic Analysis and Spatiotemporal Hotspot Identification of Urban Road Intersections. *Sustainability* **2018**, *11*, 160. [CrossRef]